Original Article

An improved model based on quantitative features of right liver lobe, maximum varices, and portal vein system measured on magnetic resonance imaging to predict oesophagogastric variceal haemorrhage secondary to hepatitis B-related cirrhosis

Bang-Guo Tan[1,2#], Zhao Tang[1#], Jing Ou[1], Hai-Ying Zhou[1], Rui Li[1], Tian-Wu Chen[1,3]^, Xiao-Ming Zhang[1], Hong-Jun Li[4]

[1]Medical Imaging Key Laboratory of Sichuan Province, and Department of Radiology, Affiliated Hospital of North Sichuan Medical College, Nanchong, China; [2]Department of Radiology, Panzhihua Central Hospital, Panzhihua, China; [3]Department of Radiology, The Second Affiliated Hospital of Chongqing Medical University, Chongqing, China; [4]Department of Radiology, Beijing YouAn Hospital, Capital Medical University, Beijing, China

Contributions: (I) Conception and design: TW Chen, XM Zhang, HJ Li; (II) Administrative support: TW Chen, XM Zhang; (III) Provision of study materials or patients: BG Tan, Z Tang, J Ou, HY Zhou, R Li; (IV) Collection and assembly of data: BG Tan, Z Tang, J Ou, TW Chen; (V) Data analysis and interpretation: BG Tan, Z Tang, J Ou, HY Zhou, TW Chen; (VI) Manuscript writing: All authors; (VII) Final approval of manuscript: All authors.

[#]These authors contributed equally to this work.

Correspondence to: Tian-Wu Chen, MD. Department of Radiology, The Second Affiliated Hospital of Chongqing Medical University, No. 74 Linjiang Road, Yuzhong District, Chongqing 400010, China; Medical Imaging Key Laboratory of Sichuan Province, and Department of Radiology, Affiliated Hospital of North Sichuan Medical College, No. 1 Maoyuan South Road, Shunqing District, Nanchong 637000, China. Email: tianwuchen_nsmc@163.com; Hong-Jun Li, MD. Department of Radiology, Beijing YouAn Hospital, Capital Medical University, No. 8 Xitoutiao Youanmenwai, Fengtai District, Beijing 100069, China. Email: lihongjun00113@126.com.

Background: In patients with hepatitis B-related cirrhosis, it is important to predict those at high-risk of oesophagogastric variceal haemorrhage (OVH) to decide upon prophylactic treatment. Our published model developed with right liver lobe volume and diameters of portal vein system did not incorporate maximum variceal size as a factor. This study thus aimed to develop an improved model based on right liver lobe volume, diameters of maximum oesophagogastric varices (OV) and portal vein system obtained at magnetic resonance imaging (MRI) to predict OVH.

Methods: Two hundred and thirty consecutive individuals with hepatitis B-related cirrhosis undergoing abdominal enhanced MRI were randomly grouped into training (n=160) and validation sets (n=70). OVH was confirmed in 51 and 23 participants in the training and validation sets during 2-year follow-up period, respectively. Spleen, total liver, right lobe, caudate lobe, left lateral lobe, and left medial lobe volumes, together with diameters of maximum OV and portal venous system were measured on MRI. In the training set, univariate analyses and binary logistic regression analyses were conducted to determine independent predictors. The performance of the model for predicting OVH constructed based on independent predictors from the training set was evaluated with receiver operating characteristic (ROC) analysis and validated in the validation set.

Results: The model for predicting OVH was established based on right liver lobe volume and diameters

^ ORCID: 0000-0001-5776-3429.

of the maximum OV, left gastric vein, and portal vein [odds ratio (OR) =0.991, 2.462, 1.434, and 1.582, respectively; all P values <0.05]. The logistic regression model equation [–0.009 × right liver lobe volume + 0.901 × maximum OV diameter (MOVD) + 0.361 × left gastric vein diameter (LGVD) + 0.459 × portal vein diameter (PVD) – 7.842] with a cutoff value of –0.656 for predicting OVH obtained excellent performance with an area under ROC curve (AUC) of 0.924 [95% confidence interval (CI): 0.878–0.971]. The Delong test showed negative statistical difference in the model performance between the training and validation sets, with a P value >0.99.

Conclusions: The model could help well screen those patients at high risk of OVH for timely intervention and avoiding the fatal complications.

Keywords: Gastrointestinal haemorrhage; liver cirrhosis; magnetic resonance imaging (MRI); portal vein

Submitted Mar 19, 2023. Accepted for publication Sep 12, 2023. Published online Oct 20, 2023.
doi: 10.21037/qims-23-353
View this article at: https://dx.doi.org/10.21037/qims-23-353

Introduction

Cirrhosis, which is characterized by liver tissue fibrosis and the transformation of normal liver structure into abnormal nodules, has been considered to the end stage of many kinds of liver damage (1). Hepatitis B virus is a prevalent aetiology of liver cirrhosis, impacting more than 300 million individuals worldwide (2,3). Portal hypertension caused by cirrhosis is associated with the formation and development of portosystemic collaterals, such as oesophagogastric varices (OV), and oesophagogastric variceal haemorrhage (OVH) has received considerable clinical attention due to the extremely high mortality rate (1,4). The prevalence of OV in the patients with cirrhosis is approximately 60–90%, and the patients with OV develop OVH at a rate of 10–30% per year (4,5). Although there has been improvement in a variety of therapies in recent years, the OVH-related mortality rate within 6 weeks after the occurrence of OVH is still over 20% (1,4,5). Therefore, timely identification of the individuals with cirrhosis at high risk of variceal haemorrhage is essential for selecting the most suitable therapy (5).

Oesophagogastroduodenoscopy is the gold standard for the detection and evaluation of OV (5). In order to evaluate the risk of OVH, most patients with cirrhosis will undergo esophagogastroduodenoscopy screening to determine the degree of OV and the presence of red wale marks, which are the endoscopic predictors of variceal haemorrhage (5,6). As an invasive procedure, esophagogastroduodenoscopy can be uncomfortable and expensive for patients with cirrhosis (7). In addition, esophagogastroduodenoscopy may cause iatrogenic OVH in the individuals with OV (2).

Being able to noninvasively predict the risk of OVH in the patients with cirrhosis may reduce the need for endoscopic screening, alleviate patient suffering, and decrease medical costs. The sixth Baveno Consensus (Baveno VI) recommends the use of noninvasive imaging tools, including magnetic resonance imaging (MRI), ultrasound, and computed tomography (CT), to predict the patients at high risk of OVH (2,8). In clinical trials, doctors consider various patient features to make a prediction, and the prediction models are the tools that combine multiple predictors by assigning relative weights to the predictors to obtain a probability or risk (9). In their studies involving hepatitis B-related cirrhosis (10-12), Liu *et al.* and Ma *et al.* investigated the feasibility of predicting OVH using the models based on CT or ultrasound features, respectively, but their prediction models only achieved moderate performance. Our previous research indicated that the morphological features of the liver lobe, spleen, and portal vein system are associated with the risk of OVH (13). Although our MRI model based on the morphological features yielded a good area under receiver operating characteristic (ROC) curve (AUC) in predicting OVH, its sensitivity was moderate (13). Additionally, the role of maximum varices size and biochemical indicators reflecting coagulation function in the occurrence of OVH was neglected in this model. In order to obtain a better performance in the prediction of OVH secondary to hepatitis B-related cirrhosis, we aimed to establish an improved novel model based on liver lobe volumes, spleen volume (SV), and the diameters of maximal OV and portal venous collaterals

obtained on MRI. We present this article in accordance with the TRIPOD reporting checklist (available at https://qims.amegroups.com/article/view/10.21037/qims-23-353/rc).

Methods

Participants

This prospective study was conducted in accordance with the Declaration of Helsinki (as revised in 2013) and was approved by the Institutional Ethics Board of the Affiliated Hospital of North Sichuan Medical College. Informed consent was taken from all individual participants.

From February 2017 to August 2020, data of 268 hospitalized participants who met the following inclusion criteria were collected from the Affiliated Hospital of North Sichuan Medical College: (I) hepatitis B-related cirrhosis was confirmed in accordance with the guidelines of the American Association for the Study of Liver Diseases (14); (II) the abdominal enhanced MRI scans, biochemical workup, and esophagogastroduodenoscopy were performed on the participants within 1 week after admission; (III) the presence of OV was endoscopically confirmed, and OVH did not occur in before or during the hospitalization; and (IV) nonselective beta-blockers, transjugular intrahepatic portosystemic shunt, or variceal band ligation was not implemented on the patients. Meanwhile, the exclusion criteria were the following: (I) space-occupying lesions of the liver or spleen (n=13); (II) previous surgery involving the spleen, liver, stomach, or oesophagus (n=10); (III) presence of diseases that could affect portosystemic haemodynamics (n=6); (IV) other comorbidities, such as primary hematologic disorders or gastrointestinal ulcers, that could cause gastrointestinal haemorrhage (n=4); (V) loss to follow-up (n=4); and (VI) unsatisfactory quality of MRI (n=1). Consequently, 230 consecutive participants with cirrhosis were enrolled into our study.

In the 230 enrolled patients, the major clinical symptoms included dull pain in the liver, abdominal distension, dyspepsia, and a feeble state. All patients were discharged with an improved condition after receiving conventional treatment. After the participants were discharged, the patients with cirrhosis were followed by telephone every 14 days for 2 years. The clinical symptoms caused by OVH, such as hematemesis and melena, would receive special attention. In addition, we encouraged the patients to contact us and report their condition if they experienced OVH-related symptoms. If the patients had suspected OVH, the presence of OVH would be confirmed via esophagogastroduodenoscopy. In each enrolled patient, our follow-up was terminated if OVH occurred or if the follow-up time exceeded 2 years. The follow-up ended in September 2022, and the median follow-up duration for the patients with OVH was 18.5 [interquartile range (IQR), 15–20] months.

Among the target individuals, 160 and 70 with liver cirrhosis were randomly divided into the training set and the validation set, respectively. During the 2-year follow-up period, 51 and 23 participants experienced OVH in the training and validation sets, respectively. In both the training and validation sets, the participants without or with OVH were further enrolled into non-OVH or OVH subgroups, respectively (*Figure 1*).

MRI techniques

In both the training and validation sets, the patient's MRI images were acquired on a 3.0 T scanner (Signa; GE HealthCare, Chicago, IL, USA) equipped with a 32-channel body coil. The routine MRI sequences included the axial single-shot fast spin-echo T2-weighted imaging (SSFSE T2WI), unenhanced and enhanced axial 3-dimensional liver acquisition with volume acceleration flexible (3D-LAVA-flex) imaging, and enhanced coronal 3D-LAVA-flex. The enhanced 3D-LAVA-flex images were acquired by administering gadolinium chelate (Magnevist; Bayer Schering, Berlin, Germany) through an antecubital vein according to a body weight-based dose of 0.2 mmol/kg at the rate of 2 mL/s, followed by a 20-mL normal saline flush. In addition, the arterial phase images, portal venous phase images. and delayed phase images were obtained at 14, 60, and 180 s after the initiation of the gadolinium chelate injection, respectively. The scan range was up to the diaphragm and down to the iliac crests. The parameters of all sequences are listed in *Table 1*.

Image analysis

The MRI data collected after initial admission were transferred to an image postprocessing workstation (Advantage Workstation Version 4.4-09; GE HealthCare) for the subsequent analyses. Compared with the arterial and delay phase images, those of the portal venous collaterals, spleen, and liver can be better observed

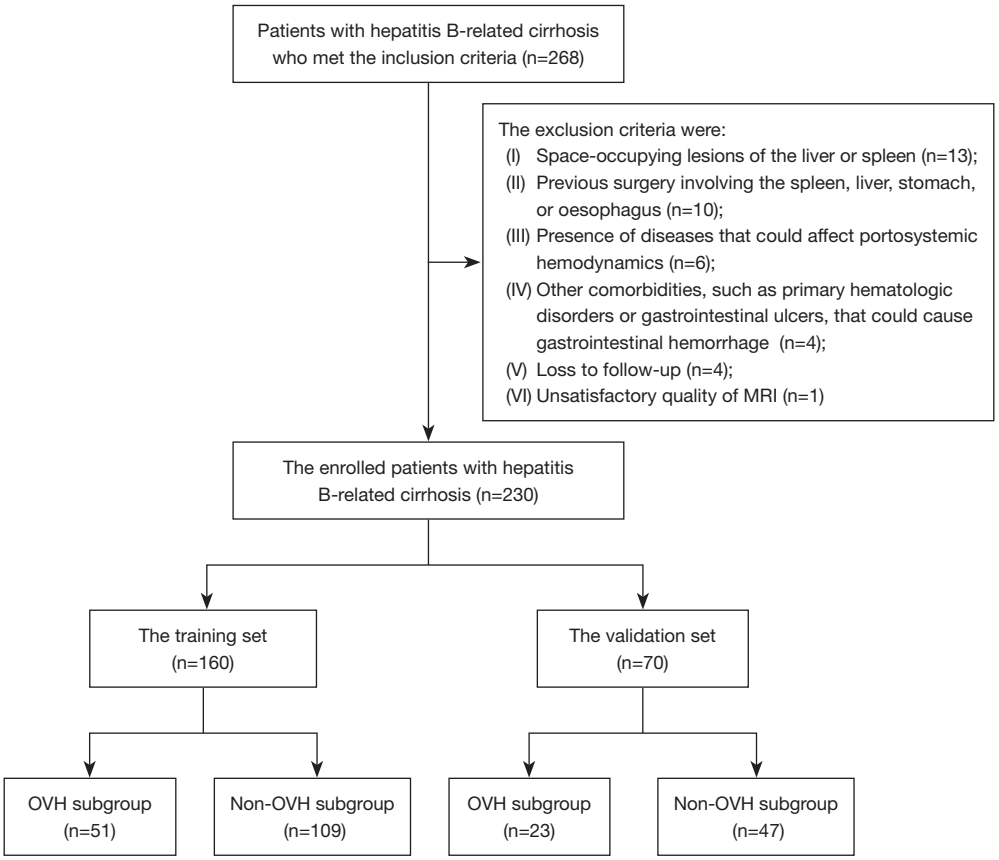

Figure 1 The flowchart for participant enrolment. MRI, magnetic resonance imaging; OVH, oesophagogastric variceal haemorrhage.

Table 1 The scan parameters of the magnetic resonance imaging sequences

Parameter	TR (ms)	TE (ms)	FA (°)	Intersection gap (mm)	FOV (cm)	Slice thickness (mm)	Matrix (mm)
Axial SSFSE T2WI	2,609	101	110	1	34×34	5.2	384×384
Axial unenhanced 3D-LAVA-flex	4.0	2.0	12	0	36×36	5.2	224×192
Axial enhanced 3D-LAVA-flex	4.0	2.0	12	0	36×36	5.2	224×192
Coronal enhanced 3D-LAVA-flex	4.0	2.0	12	0	38×38	1.3	320×224

TR, repetition time; TE, echo time; FA, flip angle; FOV, field of view; SSFSE T2WI, single-shot fast spin-echo T2-weighted imaging; 3D-LAVA-flex, 3-dimensional liver acquisition with volume acceleration flexible.

on portal venous phase images. Therefore, all the measurements were performed on portal venous phase images. The liver lobe and spleen volumes (SVs), along with the diameters of maximal OV and portal vein system, were independently measured by 2 observers (observer 1 with 4 years of experience in radiology and observer 2 with 24 years of experience in radiology) without any clinical information of the patients. There was no bias in the selection of the abovementioned variables, and each variable was considered potentially useful for the forecasting of OVH.

According to the criteria recommended by the Goldsmith and Woodburne system (15), hepatic veins in combination with hepatic fissures can divide the liver into 4 lobes (including the right lobe, caudate lobe, left lateral lobe, and left medial lobe). The details are shown in *Figure 2A*,*2B*. For accurately measuring the volumes of the 4 liver lobes, the corresponding contour of each

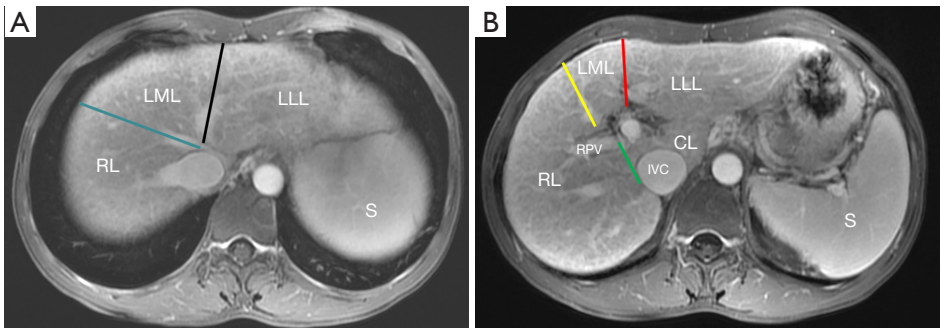

Figure 2 The boundary lines of the 4 lobes of the liver. In a male aged 50 years old without oesophagogastric variceal haemorrhage, on the level of the second hepatic portal (A), the LML appears separated from the LLL by the left hepatic vein (black line), while the RL appears separated from the LML by the middle hepatic vein (blue line). On the level of the first hepatic portal (B), the boundary line between the LML and LLL is the interlobar fissure (red line), and the boundary line between the RL from the LML is the middle fissure (yellow line). The boundary line between the RL and the CL is the green line connecting the RPV to the IVC. RL, right lobe; LML, left medial lobe; LLL, left lateral lobe; S, spleen; RPV, right portal vein; IVC, inferior vena cava; CL, caudate lobe.

liver lobe was delineated by observers slice by slice on the axial portal venous phase images, while the intrahepatic vessels and gallbladder were excluded. After delineation of corresponding contour of each liver lobe, the axial areas of the corresponding liver lobe on each slice were automatically calculated with the postprocessing workstation. The total axial area of the liver lobe was calculated as the sum of the liver lobe axial areas on each slice. The volume of the corresponding liver lobe was ultimately obtained by multiplying the slice thickness by the total axial area. Total liver volume (TLV) and 4 liver lobe volumes, including right lobe volume (RV), caudate lobe volume (CV), left lateral lobe volume (LLV), left medial lobe volume (LMV), and SV were obtained using the above-mentioned method. The percentages of individual liver lobe volumes in TLV, including the ratios of RV to TLV (RV/TLV), CV to TLV (CV/TLV), LLV to TLV (LLV/TLV), and LMV to TLV (LMV/TLV), were calculated.

The measurement points of the portal venous system diameters were acquired as follows (16,17): (I) the left gastric vein diameter (LGVD) was obtained at the measuring point 1 cm away from the insertion point of the left gastric vein into the splenic vein or portal vein; (II) the portal vein diameter (PVD) was recorded at the midposition between the bifurcation of the portal vein and the confluence of superior mesenteric and splenic veins; (III) the left portal vein diameter (LPVD) and right portal vein diameter (RPVD) were recorded at their respective bifurcation position from the portal vein; and (IV) the splenic vein diameter (SVD) and superior mesenteric vein diameter (SMVD) were obtained 10 mm away from their respective confluence. The maximum OV diameter (MOVD) was measured at the midpoint of the largest varices. The diameters of the corresponding vessel were measured perpendicular to their long axis at the measurement points. The diameters of maximal OV and portal venous collaterals were measured on coronal portal venous phase images in triplicate. The mean value of the 3 measurements was taken as the final diameter of the corresponding vein for further analyses. The original image data of the enhanced MRI were used to obtain the maximum intensity projections of the portal venous system, which were subsequently used to assist in confirming the measuring positions of the portal venous collaterals (*Figure 3*).

The 4 liver lobe volumes, TLV, SV, MOVD, and the diameters of portal venous system from observer 1 and observer 2 were used to assess the interobserver agreement of the prior measurements. To assess the intraobserver agreement, the observer 1 remeasured these parameters by using the MRI data 2 weeks after.

Statistical analyses

In order to select variables to build our prediction model, statistical analyses were performed on the SPSS version 25.0 (IBM Corp., Armonk, NY, USA) and MedCalc version 20.216 (MedCalc Software, Ostend, Belgium). A P value <0.05 indicated a statistically significant difference.

Figure 3 The maximum intensity projection image of the portal vein system. The image shows the left gastric vein (the purple arrow), portal vein (the white arrow), right portal vein (the red arrow), left portal vein (the blue arrow), superior mesenteric vein (the yellow arrow), and splenic vein (the green arrow).

The intraobserver and interobserver agreements in the TLV, 4 liver lobe volumes, SV, MOVD, and portal venous system diameters were assessed with the interclass correlation coefficient (ICC) in the training set. ICC values greater than 0.80 were indicative of excellent agreement (18).

In the training set, the statistical differences in continuous and categorical variables between the non-OVH and OVH subgroups were evaluated with the chi-squared test and Mann-Whitney test, respectively. Subsequently, the variables with statistical difference as indicated with the chi-squared test or Mann-Whitney test were enrolled in binary logistic regression analysis to determine the independent predictors of OVH. Screening of the independent predictors of OVH were performed with the forward logistic regression method of binary logistic regression analysis. The independent predictors obtained from the training set were used to construct the prediction model to predict OVH. The logistic regression model equation was obtained by multiplying each independent predictor by the corresponding regression coefficient and then adding their products together with the constant. ROC analysis was used to assess the performance of the predictive model. Finally, the performance of prediction model was validated in the validation set. We assessed the statistical difference in the model performance between the training and validation sets using the Delong test.

Results

Clinical characteristics in training set

In the training set, OVH occurred in 51 cases while the remaining 109 patients did not have OVH over the 2-year follow-up. In training set, there were no statistical differences in gender, age, only age of males, only age of females, model for end-stage liver disease score, Child-Pugh score, Child-Pugh classification, or the coagulation tests for blood clotting function between the OVH and non-OVH subgroups (all P values >0.05). The details are listed in *Table 2*.

Intraobserver and interobserver agreement in the training set

The intraobserver and interobserver agreement in TLV, the volumes of 4 liver lobes, SV, MOVD, and the diameters of the portal venous system are presented in *Table 3*. Both the intraobserver and interobserver agreements of the measurements were excellent, and all ICC values exceeded 0.80 (all P values <0.001). Due to the excellent repeatability, the subsequent statistical analyses were based on the first measurements of the first observer.

Volumes of liver lobe and spleen in the training set: OVH vs. non-OVH subgroups

The comparisons of the variables involving the volumes of liver lobe and spleen in the training set between the OVH and non-OVH subgroups are displayed in *Table 4*. The patients with OVH had lower TLV and RV than did those without OVH (both P values <0.05), whereas the CV, LLV, and LMV were not significantly different between the patients with and without OVH (all P values >0.05). In addition, the RV/TLV was lower, and the CV/TLV, LLV/TLV, and LMV/TLV were larger in the patients with OVH than in those without OVH (all P values <0.05). The SV in the patients with OVH was greater than that in those without OVH (P value <0.001).

Diameters of portal vein collateral in the training set: OVH vs. non-OVH

The MOVD, LGVD, PVD, LPVD, RPVD, SVD, and SMVD were compared between the OVH and non-OVH subgroups in the training set (*Table 4*). When compared with the non-OVH subgroup, the OVH subgroup had greater measurements for all the abovementioned parameters (all

Table 2 Comparisons of clinical characteristics

Variable	OVH subgroup	Non-OVH subgroup	P value
Gender			0.31
Male	42 (82.35)	82 (75.23)	
Female	9 (17.65)	27 (24.77)	
Age (years)	53 [43, 59]	54 [45, 63]	0.36
Only age of male	52.5 [42.25, 58.75]	52 [43.75, 60.25]	0.97
Only age of female	53 [46, 59.5]	61 [52, 64]	0.07
Child-Pugh score	9 [7, 10]	8 [6, 10]	0.15
Child-Pugh class			0.13
Class A	8 (15.69)	31 (28.44)	
Class B	26 (50.98)	40 (36.70)	
Class C	17 (33.33)	38 (34.86)	
MELD score	62.41 [59.19, 66.81]	63.30 [59.61, 70.03]	0.13
Prothrombin time (s)	16.2 [15, 17.6]	16.3 [14.55, 18.85]	0.93
Prothrombin time activity (%)	61 [47.3, 72]	66.3 [49.2, 78]	0.11
Activated partial thromboplastin time (s)	38.8 [35.4, 46.1]	39.6 [35.9, 43.75]	0.81
Thrombin time (s)	18.8 [17, 20.6]	19.4 [17.4, 20.9]	0.32
International normalized ratio	1.3 [1.19, 1.47]	1.34 [1.15, 1.61]	0.83

Data are presented as n (%) or median [25% quartile, 75% quartile]. OVH, oesophagogastric variceal haemorrhage; MELD, model for end-stage liver disease.

Table 3 The evaluations of the intra- and interobserver agreement in the measurements

Variable	Intraobserver agreement		Interobserver agreement	
	ICC value	95% CI	ICC value	95% CI
TLV	0.874	0.832–0.906	0.871	0.825–0.904
Liver lobe volumes				
RV	0.926	0.895–0.947	0.905	0.872–0.929
CV	0.938	0.916–0.954	0.920	0.884–0.945
LLV	0.945	0.925–0.959	0.928	0.901–0.948
LMV	0.901	0.867–0.926	0.885	0.845–0.915
SV	0.969	0.958–0.977	0.957	0.941–0.968
MOVD	0.821	0.756–0.868	0.815	0.755–0.861
Portal vein system diameters				
LGVD	0.911	0.877–0.935	0.904	0.822–0.943
PVD	0.884	0.844–0.913	0.860	0.814–0.896
RPVD	0.857	0.729–0.915	0.828	0.773–0.871
LPVD	0.872	0.826–0.905	0.857	0.708–0.919
SMVD	0.827	0.771–0.871	0.810	0.749–0.857
SVD	0.885	0.797–0.925	0.876	0.834–0.908

ICC, interclass correlation coefficient; CI, confidence interval; TLV, total liver volume; RV, right lobe volume; CV, caudate lobe volume; LLV, left lateral lobe volume; LMV, left medial lobe volume; SV, spleen volume; MOVD, maximal oesophagogastric varices diameter; LGVD, left gastric vein diameter; PVD, portal vein diameter; RPVD, right portal vein diameter; LPVD, left portal vein diameter; SMVD, superior mesenteric vein diameter; SVD, splenic vein diameter.

Table 4 Comparisons of the variables between the OVH and non-OVH subgroups

Variable	OVH subgroup	Non-OVH subgroup	P value
TLV (cm^3)	917.30 (697.14, 1,041.53)	1,030.20 (877.22, 1,182.99)	0.001
Liver lobe volumes (cm^3)			
RV	518.23 (387.35, 650.39)	652.47 (566.16, 801.38)	<0.001
CV	22.06 (13.24, 28.46)	18.34 (12.96, 24.54)	0.26
LLV	240.25 (153.51, 331.48)	214.75 (150.96, 285.98)	0.20
LMV	115.10 (81.42, 152.23)	110.21 (91.95, 138.74)	0.77
Percentage of liver lobe volume (%)			
RV/TLV	55.13 (50.91, 62.27)	65.96 (59.66, 72.29)	<0.001
CV/TLV	2.30 (1.64, 3.01)	1.91 (1.28, 2.33)	0.003
LLV/TLV	27.86 (20.35, 33.86)	20.64 (15.32, 26.83)	<0.001
LMV/TLV	14.14 (10.98, 15.16)	11.03 (9.41, 12.92)	<0.001
SV (cm^3)	681.80 (433.95, 909.35)	421.39 (301.35, 581.45)	<0.001
MOVD (mm)	4.90 (4.07, 6.08)	3.95 (3.57, 4.45)	<0.001
Portal vein system diameters (mm)			
LGVD	5.89 (4.01, 7.32)	3.42 (3.02, 4.08)	<0.001
PVD	16.12 (14.00, 17.29)	13.44 (12.29, 14.83)	<0.001
LPVD	10.76 (8.65, 12.18)	8.97 (7.67, 10.13)	<0.001
RPVD	10.87 (8.63, 12.32)	9.83 (8.70, 11.00)	0.04
SVD	10.73 (7.93, 12.90)	9.04 (7.93, 10.45)	0.004
SMVD	12.26 (10.83, 13.67)	11.39 (10.14, 12.50)	0.004

Data are presented as median (25% quartile, 75% quartile). OVH, oesophagogastric variceal haemorrhage; TLV, total liver volume; RV, right lobe volume; CV, caudate lobe volume; LLV, left lateral lobe volume; LMV, left medial lobe volume; SV, spleen volume; MOVD, maximum oesophagogastric varices diameter; LGVD, left gastric vein diameter; PVD, portal vein diameter; LPVD, left portal vein diameter; RPVD, right portal vein diameter; SVD, splenic vein diameter; SMVD, superior mesenteric vein diameter.

P values <0.05).

Binary logistic regression analyses and model construction in the training set

Based on above indicators with statistical differences, RV, MOVD, LGVD, and PVD [odds ratio (OR) =0.991, 2.462, 1.434, 1.582, respectively; all P values <0.05] were found to be independent predictors of OVH according to binary logistic regression analyses (*Table 5*). The model to predict OVH was established based on RV, MOVD, LGVD, and PVD and had the following equation: −0.009 × RV + 0.901 × MOVD + 0.361 × LGVD + 0.459 × PVD − 7.842.

Evaluation and validation of the model performance

In order to assess the performance of the noninvasive model in predicting OVH, ROC analysis was performed. In the training set, the prediction model could well predict OVH, with an AUC of 0.924 [95% confidence interval (CI): 0.878–0.971], along with a cutoff value, sensitivity, and specificity of −0.656, 82.4%, and 92.7%, respectively. In the validation set, the AUC, cutoff value, sensitivity, and specificity of the model were 0.926, −0.429, 91.3%, and 87.2%, respectively (*Figure 4*). Finally, the Delong test showed no difference in the results derived from the ROC analyses between the training and validation sets (P value >0.99).

Discussion

OVH is a highly fatal complication of portal hypertension that occurs in patients with cirrhosis with high morbidity and mortality. In recent years, there has been an increasing need for a noninvasive means to predicting the risk of

Table 5 Logistic regression analysis for the prediction of OVH

Variable	Regression coefficient	Standard error	Wald	P value	Odds ratio	95% confidence interval for odds ratio	
						Lower	Upper
RV	−0.009	0.002	21.247	<0.001	0.991	0.988	0.995
MOVD	0.901	0.296	9.280	0.002	2.462	1.379	4.396
LGVD	0.361	0.163	4.866	0.02	1.434	1.041	1.976
PVD	0.459	0.125	13.469	<0.001	1.582	1.238	2.021
Constant	−7.842	1.912	16.826	<0.001	<0.001	N/A	N/A

OVH, oesophagogastric variceal haemorrhage; RV, right lobe volume; MOVD, maximum oesophagogastric varices diameter; LGVD, left gastric vein diameter; PVD, portal vein diameter; N/A, not applicable.

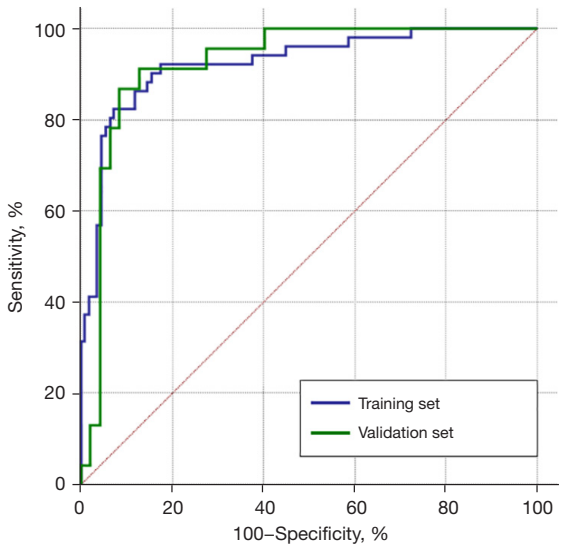

Figure 4 The ROC analyses of our model to predict OVH in the training and validation sets. ROC, receiver operating characteristic; OVH, oesophagogastric variceal haemorrhage.

OVH in patients with cirrhosis (10,13). As reported in the literature, combinations of liver and SVs as measured on CT or MRI have been considered to be potential predictors of OV and OVH in patients with cirrhosis (19,20). The diameters of portal collaterals were related to the grades of OV (5,16). Moreover, the performance of magnetic resonance portography, which is characterized by high signal-to-noise ratio, radiation-free and safety, is in line with angiography in detecting portal collaterals (17). Therefore, our study explored the feasibility of establishing an improved composite model based on individual liver lobe and SVs together with the diameters of maximal OV and portal venous collaterals to noninvasively predict OVH in the patients with hepatitis B-related cirrhosis.

As the RV in the OVH subgroup was significantly lower than that in the non-OVH subgroup, it may be an independent predictor of OVH; meanwhile, there were no statistical differences in CV, LMV, or LLV between the 2 subgroups. The variations of volumes of liver lobes may be related to the characteristic anatomical structure of the portal vein (19). The stenosis and distortion of the intrahepatic branch of portal vein caused by cirrhosis could lead to the reduction of liver blood perfusion through the portal vein, eventually resulting in the decrease of liver parenchyma volume (19,21). The intrahepatic portion of portal vein right branch is longer than the intrahepatic portions of the branches of portal vein distributed in the other 3 lobes (19). With the development of liver cirrhosis, the blood perfusion of right liver lobe is more significantly reduced, while blood perfusion of the caudate lobe, left lateral lobe, and left medial lobe is relatively adequate; this may explain the lower RV in the OVH subgroup than in the non-OVH subgroup and the lack of statistical differences in CV, LLV, and LMV observed between the 2 subgroups (19,22,23). Moreover, RV was lower in the OVH subgroup, leading to a smaller percentage of RV together with the relatively larger percentages of CV, LLV, and LMV in the OVH subgroup than in the non-OVH subgroup. Compared with those in the non-OVH subgroup, the patients in the OVH subgroup had a greater SV, which is in line with other published research (24). Splenomegaly is a common phenomenon occurring as a complication of portal hypertension in patients with cirrhosis. Splenomegaly is mainly caused by the passive congestion of spleen but may also be associated with fibrogenesis, increased angiogenesis, splenic lymphoid tissue proliferation, and inflammation (25).

Our study demonstrated that MOVD could be another

independent predictor of OVH. The risk of OVH is related to the size of OV, with larger varices posing greater risk. This finding is consistent with that of Liu *et al.* (10,11), who also detected an increase in MOVD in the patients with OVH in comparison to those patients without OVH. The increased portal hypertension leads to the increased diameter and decreased wall thickness of OV, thus resulting in increased variceal wall tension. Rupture of OV can occur in patients with cirrhosis when the variceal wall tension exceeds the elastic limits (1,11).

Furthermore, based on the larger diameters of portal vein system in the OVH subgroup, LGVD and PVD were found to be independent indicators for the prediction of OVH according to the binary logistic regression analyses in the study. The mechanisms underlying these results may be described as follows (17). As the cirrhosis progresses, the increased hepatic fibrosis and abnormal nodules lead increased intrahepatic vascular resistance and portal vein blood volume, consequently resulting in increased portal venous system pressure and dilation of the portal venous system (26-28). LGVD is a predictor of OVH, as has been demonstrated directly or indirectly in the several studies (5,16). Caraiani *et al.* reported that LGVD could be used to predict patients with OVH, with good diagnostic performance (5). Zhou *et al.* indicated that the bleeding resulting from angiorrhexis of OV, which is mainly supplied by an enlarged left gastric vein, and the LGVD could be used to discriminate between those patients at high risk of OVH from those at low risk of OVH (16). The patients with cirrhosis with large varices or variceal red wale marks as shown by esophagogastroduodenoscopy are at high risk of OVH (5). Regarding PVD as an independent predictor of OVH, we also found some supporting evidence in the literature (29,30). In Plestina *et al.*'s study, the patients with variceal red wale marks on esophagogastroduodenoscopy had significantly higher PVD than did those without variceal red wale marks (29). Meanwhile, Wang *et al.* reported that PVD could be used as the independent predictor of the patients with large varices (30).

The OVH prediction model in our study was constructed based on the independent predictors including RV, MOVD, LGVD, and PVD. The ROC analysis was performed to assess the performances of the novel composite model for predicting OVH. Our novel model had an excellent AUC of 0.924, a sensitivity of 82.4%, and a specificity of 92.7%. With a better AUC, the performance of the MRI-based model was superior to those reported in the literature based on CT or ultrasound, with AUCs less than 0.9 for predicting the occurrence of OVH (10-12). Compared with our previously published MRI model (13), the current improved MRI model had a better AUC (0.924 *vs.* 0.907) and sensitivity (82.4% *vs.* 78.6%), indicating that our current model could better screen those patients at high risk of OVH. Meanwhile, the Delong test confirmed the excellent performance of our improved model. Therefore, we can recommend that the improved model can effectively predict OVH. Once the patients are identified as being at high risk of OVH, preventive treatments, such as transjugular intrahepatic portosystemic shunt, nonselective beta-blockers, and endoscopic ligation, could be performed to reduce the risk of OVH (5). We hope that the patients at high risk of OVH as predicted by our model can receive timely preventive treatments and that unnecessary invasive endoscopic screening could be avoided in those patients at low risk of OVH.

There are a few limitations in the study that should be noted. First, the objective of our study was to predict OVH secondary to hepatitis B-related cirrhosis, and thus the logistic regression model we developed is only applicable to the cirrhosis caused by hepatitis B. Second, our study did not include the Doppler ultrasound data that could reflect the patient's haemodynamics. Third, because our study was performed with MRI and not with CT, our model remains to be validated with CT in a future study. Fourth, the effects of anterior-posterior, lateral, and oblique effects on the measurement of vessel diameters were not taken into account in this study. Finally, the external validation was not performed in this study. In subsequent research, we will collect multiple types of data to further improve our model.

Conclusions

In our study, RV, MOVD, LGVD, and PVD might be independent predictors of OVH. The model for the prediction of OVH, with a cutoff value of –0.656, was constructed based on the above 4 independent predictors and can be represented as follows: $-0.009 \times RV + 0.901 \times MOVD + 0.361 \times LGVD + 0.459 \times PVD - 7.842$. The performance of the improved model for predicting OVH was excellent, with an AUC of 0.924. We hope that our study can benefit the screening of patients with cirrhosis at high risk of OVH and enhance subsequent prevention.

Acknowledgments

Funding: This work was supported by the Key Project of National Natural Science Foundation of China (No.

61936013), and the Nanchong-University Cooperative Research Project (No. NSMC20170206).

Footnote

Reporting Checklist: The authors have completed the TRIPOD reporting checklist. Available at https://qims.amegroups.com/article/view/10.21037/qims-23-353/rc

Conflicts of Interest: All authors have completed the ICMJE uniform disclosure form (available at https://qims.amegroups.com/article/view/10.21037/qims-23-353/coif). The authors have no conflicts of interest to declare.

Ethical Statement: The authors are accountable for all aspects of the work in ensuring that questions related to the accuracy or integrity of any part of the work are appropriately investigated and resolved. The study was conducted in accordance with the Declaration of Helsinki (as revised in 2013) and was approved by the Institutional Ethics Board of the Affiliated Hospital of North Sichuan Medical College. Informed consent was taken from all individual participants.

References

1. Elzeftawy A, Mansour L, Kobtan A, Mourad H, El-Kalla F. Evaluation of the blood ammonia level as a non-invasive predictor for the presence of esophageal varices and the risk of bleeding. Turk J Gastroenterol 2019;30:59-65.
2. Yang JQ, Zeng R, Cao JM, Wu CQ, Chen TW, Li R, Zhang XM, Ou J, Li HJ, Mu QW. Predicting gastro-oesophageal variceal bleeding in hepatitis B-related cirrhosis by CT radiomics signature. Clin Radiol 2019;74:976.e1-9.
3. Ren X, Xia S, Zhang L, Li R, Zhou W, Ji R, Zhou J, Tian J, Zhan W. Analysis of liver steatosis analysis and controlled attenuation parameter for grading liver steatosis in patients with chronic hepatitis B. Quant Imaging Med Surg 2021;11:571-8.
4. Manohar TP, Patil V, Salkar HR. Combination of non-endoscopic parameters as predictors of large esophageal varices. Trop Gastroenterol 2014;35:173-9.
5. Caraiani C, Petresc B, Pop A, Rotaru M, Ciobanu L, Ștefănescu H. Can the Computed Tomographic Aspect of Porto-Systemic Circulation in Cirrhotic Patients be Associated with the Presence of Variceal Hemorrhage? Medicina (Kaunas) 2020;56:301.
6. Calame P, Ronot M, Bouveresse S, Cervoni JP, Vilgrain V, Delabrousse É. Predictive value of CT for first esophageal variceal bleeding in patients with cirrhosis: Value of para-umbilical vein patency. Eur J Radiol 2017;87:45-52.
7. Kang SH, Baik SK, Kim MY. Application of Baveno Criteria and Modified Baveno Criteria with Shear-wave Elastography in Compensated Advanced Chronic Liver Disease. J Korean Med Sci 2020;35:e249.
8. de Franchis R. Non-invasive (and minimally invasive) diagnosis of oesophageal varices. J Hepatol 2008;49:520-7.
9. Collins GS, Reitsma JB, Altman DG, Moons KG. Transparent reporting of a multivariable prediction model for individual prognosis or diagnosis (TRIPOD): the TRIPOD statement. BMJ 2015;350:g7594.
10. Liu H, Sun J, Liu G, Liu X, Zhou Q, Zhou J. Establishment of a non-invasive prediction model for the risk of oesophageal variceal bleeding using radiomics based on CT. Clin Radiol 2022;77:368-76.
11. Liu H, Sun J, Liu X, Liu G, Zhou Q, Deng J, Zhou J. Dual-energy computed tomography for non-invasive prediction of the risk of oesophageal variceal bleeding with hepatitis B cirrhosis. Abdom Radiol (NY) 2021;46:5190-200.
12. Ma JL, He LL, Jiang Y, Yang JR, Li P, Zang Y, Wei HS. New model predicting gastroesophageal varices and variceal hemorrhage in patients with chronic liver disease. Ann Hepatol 2020;19:287-94.
13. Tan BG, Tang Z, Ou J, Zhou HY, Li R, Chen TW, Zhang XM, Li HJ, Hu J. A novel model based on liver/spleen volumes and portal vein diameter on MRI to predict variceal bleeding in HBV cirrhosis. Eur Radiol 2023;33:1378-87.
14. Terrault NA, Bzowej NH, Chang KM, Hwang JP, Jonas MM, Murad MH; American Association for the Study of Liver Diseases. AASLD guidelines for treatment of chronic hepatitis B. Hepatology 2016;63:261-83.
15. Goldsmith NA, Woodburne RT. The surgical anatomy pertaining to liver resection. Surg Gynecol Obstet

1957;105:310-8.
16. Zhou HY, Chen TW, Zhang XM, Zeng NL, Zhou L, Tang HJ, Wang D, Jian S, Liao J, Xiang JY, Hu J, Zhang Z. Diameters of left gastric vein and its originating vein on magnetic resonance imaging in liver cirrhosis patients with hepatitis B: Association with endoscopic grades of esophageal varices. Hepatol Res 2014;44:E110-7.
17. Zhou HY, Chen TW, Zhang XM, Jing ZL, Zeng NL, Zhai ZH. Patterns of portosystemic collaterals and diameters of portal venous system in cirrhotic patients with hepatitis B on magnetic resonance imaging: Association with Child-Pugh classifications. Clin Res Hepatol Gastroenterol 2015;39:351-8.
18. Ma C, Liu L, Li J, Wang L, Chen LG, Zhang Y, Chen SY, Lu JP. Apparent diffusion coefficient (ADC) measurements in pancreatic adenocarcinoma: A preliminary study of the effect of region of interest on ADC values and interobserver variability. J Magn Reson Imaging 2016;43:407-13.
19. Li H, Chen TW, Li ZL, Zhang XM, Li CJ, Chen XL, Chen GW, Hu JN, Ye YQ. Albumin and magnetic resonance imaging-liver volume to identify hepatitis B-related cirrhosis and esophageal varices. World J Gastroenterol 2015;21:988-96.
20. Kim BH, Chung JW, Lee CS, Jang ES, Jeong SH, Kim N, Kim JW. Liver volume index predicts the risk of esophageal variceal hemorrhage in cirrhotic patients on propranolol prophylaxis. Korean J Intern Med 2019;34:1233-43.
21. Ozaki K, Matsui O, Kobayashi S, Sanada J, Koda W, Minami T, Kawai K, Gabata T. Selective atrophy of the middle hepatic venous drainage area in hepatitis C-related cirrhotic liver: morphometric study by using multidetector CT. Radiology 2010;257:705-14.
22. Rustogi R, Horowitz J, Harmath C, Wang Y, Chalian H, Ganger DR, Chen ZE, Bolster BD Jr, Shah S, Miller FH. Accuracy of MR elastography and anatomic MR imaging features in the diagnosis of severe hepatic fibrosis and cirrhosis. J Magn Reson Imaging 2012;35:1356-64.
23. Ito K, Mitchell DG, Hann HW, Outwater EK, Kim Y, Fujita T, Okazaki H, Honjo K, Matsunaga N. Progressive viral-induced cirrhosis: serial MR imaging findings and clinical correlation. Radiology 1998;207:729-35.
24. Pham JT, Kalantari J, Ji C, Chang JH, Kiang SC, Jin DH, Tomihama RT. Quantitative CT Predictors of Portal Venous Intervention in Uncontrolled Variceal Bleeding. AJR Am J Roentgenol 2020;215:1247-51.
25. Chen Y, Wang W, Wang H, Li Y, Shi M, Li H, Yan J. Rapamycin Attenuates Splenomegaly in both Intrahepatic and Prehepatic Portal Hypertensive Rats by Blocking mTOR Signaling Pathway. PLoS One 2016;11:e0141159.
26. Pinzani M, Rosselli M, Zuckermann M. Liver cirrhosis. Best Pract Res Clin Gastroenterol 2011;25:281-90.
27. Iwakiri Y, Groszmann RJ. The hyperdynamic circulation of chronic liver diseases: from the patient to the molecule. Hepatology 2006;43:S121-31.
28. Rahimi RS, Rockey DC. Complications and outcomes in chronic liver disease. Curr Opin Gastroenterol 2011;27:204-9.
29. Plestina S, Pulanić R, Kralik M, Plestina S, Samarzija M. Color Doppler ultrasonography is reliable in assessing the risk of esophageal variceal bleeding in patients with liver cirrhosis. Wien Klin Wochenschr 2005;117:711-7.
30. Wang L, Hu J, Dong S, Jian YC, Hu L, Yang G, Wang J, Xiong W. Noninvasive prediction of large esophageal varices in liver cirrhosis patients. Clin Invest Med 2014;37:E38-46.

Cite this article as: Tan BG, Tang Z, Ou J, Zhou HY, Li R, Chen TW, Zhang XM, Li HJ. An improved model based on quantitative features of right liver lobe, maximum varices, and portal vein system measured on magnetic resonance imaging to predict oesophagogastric variceal haemorrhage secondary to hepatitis B-related cirrhosis. Quant Imaging Med Surg 2023;13(12):7741-7752. doi: 10.21037/qims-23-353

